Invited paper presented at the Battelle
Colloquim on Fundamental Aspects of
Structural Alloy Design, Richland,
Washington, September 15-19, 1975.

LBL-4175
c.1

UTILIZATION AND LIMITATIONS OF PHASE TRANSFORMATIONS AND MICROSTRUCTURES IN ALLOY DESIGN FOR STRENGTH AND TOUGHNESS

Gareth Thomas

September 1975

Prepared for the U. S. Energy Research and
Development Administration under Contract W-7405-ENG-48

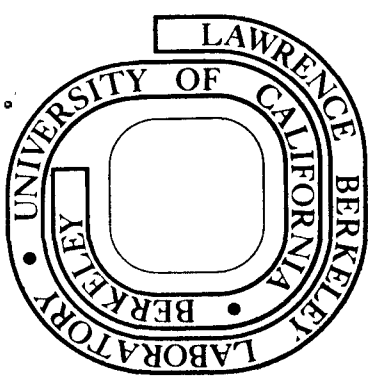

LBL-4175
c.1

DISCLAIMER

UTILIZATION AND LIMITATIONS OF PHASE TRANSFORMATIONS AND MICROSTRUCTURES IN ALLOY DESIGN FOR STRENGTH AND TOUGHNESS

by

Gareth Thomas

Professor
Department of Materials Science and Engineering
University of California
Berkeley, California 94720

ABSTRACT

The development and characterisation of microstructures resulting from phase transformations, in martensitic steels and spinodal systems, is outlined and discussed in relation to improvements in ambient temperature strength and toughness. Spinodals and martensites can both have dislocated fine grained microstructures when formed under appropriate conditions. In martensitic steels the importance of retained austenite morphology and stability on toughness at high strengths is emphasized. A method is described for improving the strength of low carbon steels by developing duplex fine grained structures of ferrite and martensite. It is suggested that coarsened spinodal alloys have good work hardening strengthening potential, if the discontinuous growth problem at grain boundaries can be overcome. Some ideas for the utilization of multiple phase transformations are also presented.

INTRODUCTION

From the viewpoint of structural alloy design the physical metallurgist is concerned with controlling microstructure and composition to produce desirable combinations of mechanical properties. The fundamental limitation of strengthening a given alloy system, is that due to

the elastic moduli. The theoretical tensile strength may be given approximately as G/20 where G is the shear modulus. If phase transformations are used to produce dislocation pinning by providing obstacles (particles or dislocations etc.) then the theoretical strength can be equated to the well known Orowan pinning model viz., $G/20 \approx Gb/_{l}$ where l is the pinning distance between obstacles, and b is the Burgers vector of the mobile dislocations. Thus at the theoretical limit $_{l} \sim 20|b| \sim$ 100Å which requires high resolution metallography for analysis. Of course there will be little or no plastic ductility at this strength level and so in design a compromise is attained so as to provide the best fracture resistance (usually large values of K_{IC} toughness) and this usually means sacrificing strength. In any case the major objective is to provide uniform obstacle distributions so that deformation by slip will occur uniformly so as to minimise local stress concentrations. Phase transformations leading to heterogeneous distributions of precipitates are thus usually undesirable.

In this paper the utilization of two major transformations are discussed viz. martensitic and spinodal since these currently show great potential for manupulation and application of novel approaches to microstructure-property control. Ordered alloys (including ordered matrix solid solutions, interstitial ordering and embrittlement) will not be discussed. The properties to be considered are tensile strength and fracture toughness (as measured by K_{IC} and charpy) relevant at ambiant temperatures, and the alloy systems described are experimental ones designed in an attempt to facilitate basic understanding of the problems involved.

A comprehensive review of this rapidly developing field of research is not intended but rather a summary of results and ideas of current work in my group. Emphasis is also placed on the need for detailed and quantitative electron metallographic analysis so as to properly characterise microstructure even though this may not directly assist in elucidating the reaction mechanisms. An important aspect not covered in this paper (see the one by McMahon in this book), is the chemical analysis of small volumes to which new electron optical techniques such as Auger analysis and micro-x-ray analysis using scanning-transmission instruments are being applied. Such work is essential for developing commercial alloys since impurities alone may be the chief limitation on performance.

2. Some Problems of Uniformity of Microstructure

As mentioned above a major concern for microstructure-property control is that of uniformity of microstructure and the need to identify desirable and undesirable features. The fundamentals of the mechanisms of phase transformations must therefore be understood and the microstructures properly and quantitatively characterised. A brief outline of some of these factors follows.

a) Nucleation and Growth Systems

For nucleation and growth (N&G) transformations it is necessary to consider both homogeneous and heterogeneous reactions. In the absence of an applied stress, the free energy ΔF_n associated with nucleation has been expressed by (e.g. Cahn (1)) $\Delta F_n = -\Delta F_v + \Delta F_s \pm \Delta F_e$ where ΔF_v is the volume free energy, ΔF_s the surface free energy and ΔF_e the strain energy (this is negative in heterogeneous nucleation, e.g., at

dislocations).[2] In order to produce homogeneous nucleation, large supersaturations are needed, i.e. the ΔF_v term must dominate. In systems where quenching from the single phase region precedes aging, inhomogeneities can be introduced e.g., large vacancy supersaturations and additional dislocations. Subsequent aging produces microstructures that may then not be uniform e.g., precipitation at grain boundaries (due to the influence of the surface and strain energy terms and the higher diffusion rates), precipitate-free-zones and precipitation on defects in the matrix. In some cases different phases may appear, as is well known for Al-Cu base alloys where θ" occurs in the matrix, θ' on dislocations and θ' or θ at grain boundaries in the same alloy on aging to near maximum strength.[2] Thus control of uniform microstructure is very difficult, especially if it is to be accomplished by only simple heat treatments. The Al-Zn-Mg system (commercial 7075) is a good example of one of the potentially highest strength Al alloys which is limited by the heterogeneity of precipitation and a compromise between toughness and strength can be achieved by overaging. However, some experimental advances have been made with complex multiple treatments including thermal-mechanical treatments, especially for alleviating grain boundary heterogeneities.[3,4]

b) Spinodal systems

For perfectly homogeneous phase separations, such as in spinodals where the above equation does not apply, uniformity of structure is attained immediately after the transformation and can be attained by direct cooling from the solution temeprature.[5-8] The problem that arises in the post-nucleation period is that coarsening rates may differ

at boundaries and within the matrix. Figures 1, 2 compare light optical and transmission electron optical micrographs of the structures after advanced aging in a Cu-Ni-Fe alloy. It might appear from Fig. 1 that a new type of grain boundary process has occurred, but a recent detailed study of the morphology (Fig. 2), crystallography, and kinetics of aging[9] has demonstrated that this effect is due to accelerated coarsening, generally only at large angle boundaries, and accompanied by grain boundary migration. Since for this alloy system the formation of the grain boundary product is growth controlled, it cannot be due to a discontinuous or cellular reaction, both of which are nucleation controlled.[8] It is also interesting that the toughness of this CuNiFe spinodal alloy decreases[10] as a result of this grain boundary coarsening. A detailed study of this coarsening problem is in progress so that attempts can be made to solve the boundary problem by a fundamental approach to design, with changes in alloying and/or heat treatment e.g. to lower grain boundary mobility.

During spinodal coarsening dislocation networks form at the interphase boundaries to relieve the coherency strains when coarsening proceeds and the phase compositions approach their equilibrium levels. An example for CuNiFe is shown in Fig. 3. In this way walls of dislocations are generated periodically so providing a regular "dispersion" of cell boundaries which should be good sources of strengthening (Sec. 3c) However, the toughenss will be limited if grain boundary effects such as those described above cannot be overcome.

Despite the great potential for utilizing spinodal reactions to produce tough, strong alloys, the amount of work on spinodal systems has

so far been extremely small especially from the structure-property viewpoint (Sec. 3), by comparison to the efforts expended on examination of transformations of other kinds. The development of alloy theory to allow prediction of spinodal transformation in several component systems is clearly desirable.

c) Martensitic Systems in Iron Based Alloys

The martensitic transformation can also produce a uniform microstructure provided that the internal substructure produced by the transformation shear and subsequent accomodation (slip or twinning) is unique.[11,12] Figure 4 shows electron micrographs typical of the dislocated and twinned martensites that are found in quenched iron based alloys.

It is now established that martensitic carbon steels have poor K_{1C} toughness if the structure is twinned (say approximately 10% or more, i.e. when the carbon content exceeds ~0.3%). In our alloy design program, studies are being done on high purity, basically, but not exclusively, ternary Fe-C-X alloys, which are vacuum melted. The X refers to alloying elements, Cr, Mo, B etc. These alloys, whilst serving as model systems so as to provide basic information on the role of alloying elements on microstructure, strength and toughness by minimising well known problems of impurity embrittlement, have also turned out to provide excellent properties even in the untempered condition (see Fig. 5a), which is advantageous economically. Figure 5b shows results of current work on grain refined dislocated martensites[14] in Fe-1%Cr-1%Mo-0.3%C. These data can be compared to those for Fe/Mo/C alloys shown in Fig. 5a. It should be noted that these properties

compare very favorably with commercial high alloy steels e.g. the 18%Ni maraging type.

d) Microstructure Control for Martensitic Structural Steels

As a result of basic studies on the role of alloying and microstructure on mechanical properties (reviewed in ref. 13) some guidelines can be given for designing strong, tough steels. These are

1. Obtain dislocated martensite with minimal twinning: This is largely determined by carbon content and total alloy content, which both affect the Ms temperature. Thus a lower limit of Ms of about 350°C is recommended (max. carbon ~0.4%). This structure can be achieved by direct quenching and sufficient hardenability is obtained by adding substitutional elements such as Cr, Mo etc; i.e. the X component in the Fe-C-X series. Thus the total amount of solute must be controlled to control Ms-Mf and hardenability. Hardenability is needed to prevent undesirable structures resulting from diffusional products, (e.g. pearlite, upper bainite). Some autotempering may occur on quenching but this should not lead to embrittlement provided the carbides only nucleate within martensite and not at boundaries. In this regard lower bainite may also be a desirable structure.[13]

2. A composite structure wherein the martensite (or lower bainite) is surrounded by continuous thin films of austenite appears to greatly benefit K_{1C} toughness at high strengths (Figs. 5, 12). These films can again be obtained by control of composition and heat treatment through a knowledge of transformation kinetics and effects of alloying additions. The stability of this austenite is important e.g., on tempering (even auto-tempering) it if decomposes to ferrite and carbide the undesirable

boundary carbide morphology occurs resulting in embrittlement.[28] The addition of alloying elements such as Al and Si are beneficial in this regard (see also the paper by Parker and Zackay in this book). If the austenite films are mechanically unstable they may transform under stress. If they transform to martensite (so called trip mechanism) this could be a useful toughening reaction during crack propagation.

It is the formation of grain boundary carbides that probably limits the possibility of using continuous cooling to directly transform austenite to a mixture of dislocated ferrite and carbides (auto-tempered martensite or lower bainite) which can also be done to produce a dispersion strengthened alloy steel (see e.g. Honeycombe, ref. 15). Current work on bainite[16] confirms the viewpoint that upper and lower bainite form by different mechanisms and should be represented by separate curves in TTT diagrams. This means that careful evaluation of transformation kinetics and microstructure is needed if a particular alloy system is to be fully exploited; this is especially true for existing commercial alloys.[17] It cannot be emphasised too strongly that much of the enormous terminology that has developed to describe the microstructures in steels has arisen from inadequate resolution (Troostite, Sorbite, etc) and has lead to confusion. High resolution electron microscopy is absolutely essential to characterise and thus clearly specify the microstructure, e.g., to distinguish upper and lower bainite, and to differentiate narrow bands of inter-lath austenite and cementite (Sec. 4c). Furthermore, whilst grain/packet/lath/phase boundaries in martensitic steels provide strength by providing effective barriers to dislocation motion, the exploitation of this potential

strengthening source without loss of toughness, requires careful design of heat-treatments to avoid boundary decoration by brittle precipitates or other heterogeneities.

In summary, although both martensitic and spinodal reactions can produce uniform microstructures, and provide dislocations without external plastic deformation, grain boundary effects are still probably the most important factors determining the mechanical properties of the alloys.

3. Spinodal Transformations and Alloy Design

The attractiveness of the spinodal transformation stems from the uniform, homogeneous, usually periodic microstructures that are produced (see e.g., the matrix regions in Fig. 2). Since a spinodal microstructure can be characterized by the wavelength and amplitude of its periodic composition modulations (Fig. 6) these parameters must be accurately determined for correlation with desirable properties.

a) Coherent Spinodal Products

From a survey of the available experimental data for several alloy systems which appear to decompose spinodally[6,7,18-24] it is obvious that a universal theoretical explanation for strengthening in spinodal alloys has not been found. When correlations have been attempted, it is generally agreed that the yield strength σ_y is not dependent upon wavelength λ during the time the spinodal product remains coherent. The results obtained on the Cu-Ni-Fe spinodal alloys,[6,7] which have served well as a model system, have shown that the yield strength of the coherent spinodal depends on the composition difference Δc between the two phases which is related to their difference in lattice parameters,

Δa, (Fig. 6), independently of the wavelength and volume fraction. If the elastic constants of the two decomposed phases are nearly the same, then, based on a theoretical treatment by Dahlgren,[24] the maximum yield stress is given by $\sigma_{y_{max}} \propto \Delta a_o$ where Δa_o is the difference in lattice parameters of the two spinodal products at their extreme tie-line compositions. For the same condition the yield stress is predicted to be independent of wavelength and volume fractions of the spinodal product. When the elastic constants of the phases show appreciable differences, then some volume fraction dependence is indicated in the yield stress.

Dahlgren[24] was careful to point out that while the decomposing phases are still coherent, the "extreme" compositions do not correspond with the limits of the miscibility gap, so that the phases are metastable.

b) Semicoherent Spinodal Product

During spinodal coarsening the change in compositional differences Δc maximises as the equilibrium tie line conditions are attained, and so the yield stress -Δa relationship no longer holds. At this stage of transformation, coherency is lost and interfacial misfit dislocations are generated (Figs. 3,7). The Burgers vectors of these dislocations in CuNiFe alloys are a/p<110>(or a/q<100> in other cubic alloys)[25] where the magnitudes of p and q depend on the misfit (normally p = 2, q = 1).

Thus overaging has introduced a regular array of dislocation walls. Upon plastic deformation the slip dislocations must overcome the interactions with the dislocations at the interface (Fig. 7) or even possibly push the interface dislocations out of the interface. The overall interaction distance is nevertheless λ , the compositional wavelength,

and slip will occur preferentially in the softer phase. If the volume fractions of the two phases are unequal (Fig. 6) the yield stress is expected to be volume fraction dependent.

c) Potential for Strengthening Semicoherent Spinodals

From the foregoing it is clear that the overaged semicoherent spinodal alloy systems are attractive from the dispersion and work hardening viewpoint, especially if they can be produced by direct slow cooling from the solution temperature. On straining, a glide dislocation in such a material will experience two types of obstacles: (i) Regions of elastic inhomogeneity, and (ii) Periodic arrays of dislocations that delineate the regions of elastic inhomogeneity (Fig. 3).

Assume a dislocation source exists at the interface and a dislocation moves a distance $\sqrt{2}\lambda_A$ in phase A before coming to the next interface, and that the system like CuNiFe is fcc (Fig. 7). At this point the slip dislocation must interact with the wall or forest of the two sets of interface dislocations. Thus, a strong interaction is expected at these junctions. Once this interaction is exceeded, the dislocation must either penetrate into the next phase B and travel a distance $\sqrt{2}\lambda_B$ before again becoming pinned due to interface interaction, or find a route through an adjoining "particle" of phase A so that slip essentially occurs entirely in phase A (assuming phase A is softer than phase B). A possible example of this behaviour is visible in Fig. 3.

Work on dispersion hardened materials, for which there are several contributions to the total hardening, suggests[26] that the independent contributions should be summed as:

$$\tau_{Total} = \sqrt{\tau^2_{el.\ inhom.} + \tau^2_{array}}$$

As the periodic arrays are stable because they consist of structural dislocations, the interfaces can be considered similarly to grain boundaries, in which case a Hall-Petch type of strengthening would be expected, i.e. yield strength is proportional to $(\lambda)^{-1/2}$. Basically the question of dislocation motion is determined by the energy of the dislocation in the two phases viz., line energy $T \alpha G b^2$, and $T_A \sim G_A b_A^2$ in phase A and $T_b \sim G_B b_B^2$ in phase B. Since $|b_A| \simeq |b|_B$ the important term is the shear modulus and dislocation motion in phase B will be negligible if $G_B >> G_A$.

It should be emphasized that the attractiveness of a spinodal system for this type of strengthening depends on the manner in which the dislocation substructure is produced and the way in which λ can be controlled. Thermal treatment alone, including perhaps merely furnace cooling, may induce the formation of regular high density dislocation arrays at the interphase interfaces, without the need for mechanical processing of any kind. The limitation in exploiting these alloys rests with any grain boundary problem, such as the accelerated coarsening in CuNiFe described in Sec. 2(b).

d) Summary

From an alloy design point of view, the problem of identifying the strengthening mechanisms in spinodal alloys must be solved before they can be effectively exploited. It appears that the only way to circumvent the embrittling grain boundary effects so that the potential strengthening due to semicoherent spinodals may be studied, is by analysis of single crystals. Detailed electron microscopy analysis can then be used to determine the nature of any slip-interfacial dislocation reactions, slip-

traces, etc., leading to an understanding of the strengthening process throughout the entire aging sequence, including any changes in strengthening mechanism. Finally, fracture toughness measurement of polycrystals must necessarily be included in any study, even for systems in which heterogeneous grain boundary precipitation may have been avoided, since lamellar structures, particularly spinodals, are well known to coarsen discontinuously.[9]

4. Exploitation of Martensitic Transformations

a) Strength of Martensite

The strength of martensite is determined principally by the carbon content in solution and the toughness by the microstructure, which in turn depends upon composition and heat-treatment. Experimental steels have been designed to obtain improved properties merely by transformation to dislocated martensite as outlined in Sec. 2(d). This transformation provides one of the most efficient means of obtaining uniformly dislocated microstructures, and tempering is not required to obtain desirable toughness at ambient temperatures as shown in Fig. 5(a).*

Although the strength can be increased merely by increasing the carbon content, beyond about 0.4%C, steels have low toughness. A simple linear hardening theory for polycrystals due to

---

*However, although K_{1C} is fairly high, in these experimental steels (Fig. 5) the critical plastic zone size is very small if the strength is also high e.g. at a K_{1C} of 80 ksi $\sqrt{\text{ins}}$ and a strength of 300,000 psi, the critical value of plastic zone size is only ~0.01 ins based upon the McClintock criterion (loc. cit).

interstitial carbon is given by the well-known Nabarro theory $\tau_c = G\varepsilon^2 C$ where τ_c = shear yield strength, G = shear modulus, ε = misfit and C = atomic fraction of carbon. This equation predicts a strength of ~G/300 at 0.35%C. The other important strengthening parameter is the dislocation density, and since the martensite is essentially work-hardened as a result of the high dislocation content resulting from the transformation, the contribution from these dislocations can be written in terms of a flow stress $\tau_f \cong G.b\sqrt{\rho}$ where b = Burgers vector, ρ = dislocation density.

Thus to double the strength due to this contribution, the dislocation density must be increased by at least a factor of 4. Such high dislocation densities may be achieved by deformation e.g. ausforming.

b) Limitations of Carbon Content: Design to Eliminate Quench Cracking (Experimental Fe-4Cr-0.4%C Steel)

Since one of the most economical ways of increasing the strength of a steel is to raise its carbon content, it is worth considering what might be done to overcome the limitation of this procedure, namely the onset of embrittlement due to quench cracking at the prior austenite grain boundaries, which occurs even in relatively high purity alloys. We have recently investigated this problem in an experimental Fe/4Cr/0.4%C steel[27], since a similar steel but with a lower carbon content viz., 0.35%, has excellent combinations of high strength and toughness even in the untempered condition (See Fig. 5a)[28]. In order to eliminate undesirable alloy carbide morphologies from the microstructure of these Fe/Cr/C alloys (for example, at prior austenite grain boundaries), it was necessary to austenitise the Fe/4Cr/0.4C steel at high temperature (>1000°C), but this practice led to intergranular cracking during the quench in either oil or water (Fig. 8a). After such high temperature treatments the grain size was large (>300μ,

i.e., ASTM 0.5) (Fig. 8a) and the microstructure contained extensive twinning but little evidence of auto-tempering (Fig. 8b) while scanning electron microscopy showed largely intergranular fracture (Fig. 9A). Based on the study of the effect of the heat-treatment variables on the intergranular cracking tendency[27], it was concluded that the amount of carbon in solution (γ) and martensite packet size* are the two most important factors influencing cracking tendency, viz., an increase in either causes an increase in cracking. In order to achieve desirable fracture toughness properties so that the steels can be utilized in engineering applications, it is essential to austenitize at a high enough temperature to dissolve all carbides. At the same time, in order to avoid quench cracking at high levels of carbon in solution, it is necessary to obtain a small grain size. Clearly, for martensitic structures these requirements cannot be achieved in a single heat-treatment.

Multiple heat treatments were then designed[27] and the results are summarised in Fig. 9. The corresponding microstructures and mechanical properties are summarised in Figs. 8 and 10 respectively.

These results show that by ideally combining the benefits of high temperature austenitization and small grain size in the double treatments, the resulting mechanical properties of quenched structures are optimized and are superior to those of conventionally produced lower bainite in the same steel as shown in Fig. 10. Since it is proposed that intergranular quench cracking results from the accommodation of strain generated by impingement

---

* A martensite packet is defined as a group of dislocated martensite laths usually slightly misoriented or twin related.

of two or more growing martensitic packets at the grain boundaries, a small martensite packet size (i.e., small austenite γ grain size), auto-tempering and the establishment of good intercrystalline cohesion (by elimination of undissolved carbides at the boundaries) are some of the factors which contribute favorably to a solution of the intergranular quench crack problem.

c) Retained Austenite Identification and Significance in Quenched (and Tempered) Steels

As discussed earlier the results on martensitic steels have shown that retained austenite has an extremely important effect on fracture toughness (measured by K_{IC} and Charpy) at a particular strength level. For example at 250,000 psi quenched strength levels the K_{IC} value for Fe/Cr/C was 70 ksi $\sqrt{\text{ins}}$ yet only 54 ksi-in$^{1/2}$ for Fe/Mo/C, (Fig. 5a) i.e. the Fe/Cr/C steel is much tougher by the K_{IC} criterion. Detailed electron metallography and diffraction has shown that in the Fe/Cr/C steel,[28] continuous sheets or fibers of inter-lath austenite are present, whereas if present they were not resolved in the Fe/Mo/C steel.[31]

Since such thin layers of austenite are not detected by x-ray analysis and since the analysis is not a trivial matter it is worth emphasing the need for proper characterisation, using electron microscopy and diffraction. Firstly in most cases the volume fraction of retained austenite in structural steels is small, and hence the austenite diffraction reflections are often weak. Careful tilting in order to bring the austenite films into a strong diffracting condition and the matrix into strong transmitting condition is necessary to enable the austenite diffraction spots to be recognized. Secondly, in most structural steels auto-tempering occurs during quenching and so the diffraction pattern is further complicated by the presence of extra reflections from the carbide particles. A clear

distinction of austenite reflections from carbide reflections is thus not straightforward due to the similar spacings occuring in the patterns, and because spherical aberration limits the spatial resolution in selected area diffraction to ~2μ at 100 kV although this is greatly improved at higher voltages. A choice of appropriate orientation for unambiguous characterization of structure is thus necessary. Analysis[32] has shown that a <111> martensite orientation is suitable and a constructed pattern is shown in Fig. 11. This pattern is to be compared with an actual analysis shown in Fig. 12 for which the (200)γ reflection spot was used to obtain the dark-field image of retained austenite films. Whilst the amount of retained austenite can vary with treatment[27,33] detection now seems to be quite general[32,35] even in low carbon steels (0.1%) as revealed by the sophisticated electron microscopy analysis just described and strongly recommended for all such studies.

d) Control of Untransformed Austenite: Stability

Current work shows that isolated particles of retained austenite are not as beneficial as continuous films (Fig. 12, 13) suggesting that austenite may act as a crack stopper at the lath boundaries, or that it promotes crack branching along the boundaries, perhaps in a similar manner to fracture in certain fiber composites[34]. Such a mechanism could explain the fractographs often observed in our steels (Fig. 13) as was discussed earlier (Sec 2d). It has been observed that increasing the austenitizing temperature can increase the toughness[17]. Current work on Fe/4Cr/0.3%C steels shows that increasing the austenitizing temperature from 870°C to 1200°C increases the value of K_{IC} from 64 ksi $\sqrt{in}$ to 82 ksi $\sqrt{in}$, although the properties seem to be optimised by 1100°C treatment.

The criterion for the critical value of the plastic zone size discussed by McClintock in his paper (loc. cit.) is $r_c = 1/2\pi[K_{IC}/Y]^2$ (where Y has some value between the yield and ultimate tensile strength). Thus the corresponding values for r_c are 250μ after the 870°C austenitizing and ~430μ after the 1200°C austenitizing, taking Y as the UTS (250 ksi and 200 ksi respectively). Since the grain size increases from 30μ to 250μ with this increase in austenitizing temperature, it may be that the grain size is the most important factor determining crack propagation (as measured by K_{IC}). Since increasing grain size also increases hardenability, there may also be an effect due to retained austenite (see Parker and Zackay loc. cit). Carbon segregates to the austenite and could stabilize it against transformation (due to a lower M_s locally). More experiments are now in progress to obtain more quantitative data on these variables as well as obtaining charpy data. The influence of austenitizing temperature on austenite carbides and martensite substructure which already has been shown to be important for the Fe/4Cr/0.4C steels discussed above,[27] will receive special emphasis.

With reference to the observed differences in toughness between the Fe/Cr/C and Fe/Mo/C steels (Fig. 5a), the greater amount of retained austenite in the former alloy is to be expected since Mo has a very strong effect in limiting the austenite range of stability (~2% Mo compared to ~13%Cr), so that each alloying element may have a different effect on the amount and possible distribution of retained austenite. Alloy design programs to study this problem are also in progress at Berkeley.

e) Summary

In this section it has been shown that simple control of composition and heat treatment to produce dislocated martensite and continuous films

of retained austenite leads to excellent combinations of ambient strength and toughness, whereas interlath carbides lead to embrittlement (Fig. 13). Also the limitation due to quench cracking on increasing carbon concentration to increase strength of martensite steels, can be alleviated by multiple, though probably expensive, heat treatments. Further work is necessary to study in more detail the effects of alloying to control retained austenite and processing to achieve grain refinement.

The martensitic transformation can also be exploited as a possible means of strengthening softer phases by controlling the transformation (either thermally by control of M_s temperature or mechanically by control of M_d) so as to form a dispersion of martensite e.g. with ferrite. It is known that duplex austenitic-martensitic alloys, e.g. 304 stainless steels, can be strengthened this way. Furthermore, the flow stress has been found to vary linearly with volume fraction of martensite[35] irrespective of the way that martensite was produced. In the following section an approach is described in which martensite is used as a strengthening dispersion with ferrite, in low carbon steels.

5. Duplex Structures and Strengthening of Low Carbon Steels

Whilst a considerable effort in research and development has gone into improving the strength and toughness of medium and high carbon steels much less effort has been directed towards understanding more completely the structure-property relationship in low carbon steels. With the increasing problem of materials and fuel shortages, however, there is now an urgent need for design engineers to effect weight reductions in transportation systems such as automobiles by achieving economical increases in strength of steels or new alloys. Interest is developing in high strength

low alloy steels, but room exists for improvements in plain carbon steels e.g. 1010.

For plain low carbon steels several approaches have been used in the past, e.g., rapid heating and cooling cycling through the austenite transition temperature for grain refinement[36]. However, if the final transformation product is a mixture of ferrite and pearlite, the strength level is not as great as is required. On the other hand if the cycling is done so as to attempt to produce 100% martensite, the ductility is poor and undesirable microstructures (e.g. upper bainite) can often result, due to the low hardenability.

In considering commercial automobile steels e.g., INNA and 1010 (basically Fe-0.5Mn-0.1C with INNA having 0.01N also), a novel way of thermal cycling which involves annealing in the two phase ($\alpha + \gamma$) field has been used. This heat treatment and subsequent cycling treatment is compared to conventional cycling for grain refinement in Fig. 14. The initial austenitizing treatment consisted of annealing in argon at 1100°C (30 mins.) so as to dissolve all carbides followed by ice brine quenching to obtain 100% martensite as the starting microstructure (Grange[36]). Details of the experimental conditions and range of cycling treatments investigated will be published elsewhere[39], but the initial grain size was ASTM #2 (~80μ) which is refined by the cycling process, e.g. after the second cycle, the grain size is ~18μ.

By holding in the ($\alpha + \gamma$) temperature range, the α and γ phases will attain the compositions specified by the tie line corresponding to the holding temperature. The alloy will then consist of low carbon ferrite and higher carbon austenite. Upon quenching, the austenite transforms

to martensite which electron microscopy shows to be dislocated (see Fig. 15). The ferrite which does not transform back to austenite during the reheating to the [$\alpha + \gamma$] field contains sub-boundaries formed as a result of dislocation generation and rearrangement during cycling. These walls (~1μ apart) become sites for carbide (or nitride) precipitation on tempering, which can be a further source of strengthening.

This method of using the two phase ($\alpha + \gamma$) field has also been utilized by Jin et al.[37] for Fe/Ni and maraging steels and Snape and Church[38] for low alloy steels. However, the transformation behaviour and beneficial results obtained for the 0.5Mn/0.1C steels differ from those in the higher alloy steels.

The effects of the ferrite-martensite mixtures on the yield strength and ductility (% elongation) are shown in Fig. 16. This graph also contains the commercial specifications for the "INNA" steel. It can be seen that the new heat treatments described here can double both the yield strength, and also the tensile strength (due to the greater work-hardening capability) at an acceptable uniform elongation level of 10%. The method could be useful as a finishing treatment for improving strength (i.e. after forming). The improved mechanical properties can be interpreted in a manner used for duplex structures such as fiber composites, for the condition that the microstructural consitituents (ferrite and martensite) are equally strained. The flow stress can then be expressed as $\sigma_f = \sigma^{\alpha} f(\alpha) + \{1-f(\alpha)\}\sigma^m$ where σ^{α} = flow stress for ferrite, σ^m = flow stress for martensite, $f(\alpha)$ = volume fraction ferrite. Such a relationship is in agreement with the data in Fig. 16. It should be noted that σ^{α} is determined principally by the ferrite grain size and whether

or not it is also precipitation hardened. As discussed earlier, σ^m is determined by the carbon content, which can be varied by the annealing temperature in the α-γ range (Fig. 14).

These results indicate the improvements that can be made in these low carbon steels. Since several million tons are produced each year, some savings in material are clearly possible if these strengthening treatments can be adopted economically by industry.

6. Concluding Remarks: Use of Multiple Transformations

Steels are systems where several transformations occur during production e.g. during the martensite transformation, precipitation of carbides can occur simultaneously or consecutively. However, much more potential exists for combining more than one type of phase transformation in the same alloy system, especially as a means for eliminating mechanical stages in processing to produce microstructures with useful combinations of properties. For example, consider the ausforming treatment (see Fig. 17). This process involves deformation of metastable austenite during which heterogeneous nucleation of carbides on dislocations occurs[40]. On quenching, the carbon depleted austenite transforms to martensite, and provided that the martensite is dislocated ($C \lesssim 0.3\%$), the steel has greater toughness and strength than is obtained by conventional martensitic transformation. This approach is limited by the austenite transformation kinetics in that the pearlite and bainite transformations need to be well separated. However, similar results can be obtained without the deformation if precipitation can be induced in austenite prior to transformation. Examples of this process include ausaging FeNiTi type alloys to precipitate Ni_3Ti[41] or spinodally decomposing CuNiFe prior to quenching to form

martensite[42]. For these processes to be effective it is essential to produce dislocated martensite so that dislocation multiplication can occur at the precipitates during the martensitic transformation (Fig. 17). The composition of the alloy limits the usefulness of multiple treatments since it determines whether or not martensite can be formed (athermally below Ms or by deformation below Md), but nevertheless much can be done to explore these ideas further.

ACKNOWLEDGEMENTS

This work was done under the auspices of the United States Energy Research and Development Administration through the Inorganic Materials Research Division of the Lawrence Berkeley Laboratory. I want to thank members of my research group for their invaluable contributions and for providing me with the data and illustrations; their names are given in the pertinent Figure Captions. I also wish to thank various companies especially Inco, Republic Steel, Climax Molybdenum and Daido Steel who have generously donated alloys made to our specifications. I am grateful to Dr. Noel Kinnon for his critical, helpful review of the manuscript.

REFERENCES

1. Cahn, J. W.: Acta Met., 5: 169 (1957).

2. Nicholson, R. B.: "Phase Transformations in Metals", Amer. Soc. Metals, p. 269, 1970.

3. Thomas, G.: J. Inst. Metals (London), 89: 253 (1960-61).

4. Lorimer, G. and R. B. Nicholson in "Mechanisms of Phase Transformations", Inst. of Metals (London) p. 36 (1969). Lorimer, G. W., M. J. Nasir, R. B. Nicholson, K. Nuttall, D. E. Ward and J. R. Webb: "Electron Microscopy and Structure of Materials", G. Thomas (ed.), p. 222, Univ. Calif. Press, (1972). See also P. Doig, J. Edington and M. H. Jacobs: Phil. Mag., 31: 285 (1975).

5. de Fontaine, D.: "Ultrafine-Grain Metals", J. J. Burke and V. Weiss (eds), p. 93, Syracuse Univ. Press, 1970.

6. Butler, P. and G. Thomas: Acta Met., 18: 347 (1970).

7. Livak, R. and G. Thomas: Acta Met., 19: 497 (1971).

8. "Phase Transformations" Amer. Soc. Metals (e.g. p. 487) 1972.

9. Gronsky, R. and G. Thomas: Acta Met., (In Press) (1975). Lawrence Berkeley Laboratory Report #3523, Jan. 1975.

10. Livak, R. J. and W. W. Gerberich: "Electron Microscopy and Strength of Materials", G. Thomas (ed.), p. 647, Univ. of Calif. Press 1971.

11. Wayman, M.: "Modern Diffraction and Imaging Techniques in Materials Science", S. Amelincx et. al. eds, p. 187, North Holland Press, 1970.

12. Thomas, G.: Met. Trans., 2: 2372 (1971).

13. Thomas, G.: Iron and Steel Intern., 46: 451 (1973).

14. Chen, Y.-L, Ph.D. thesis in progress, University of California, Berkeley.

15. Honeycombe, R. W. K.: "Structure and Strength of Alloy Steels", Climax Molybdenum Co. publication, 1975.

16. Huang, D. H.: Ph.D. Thesis, Univeristy of California, Berkeley, Lawrence Berkeley Laboratory Report #3713, 1975.

17. Parker, E. R., and V. F. Zackay: "Alloy Design", J. K. Tien and G. S. Ansell (eds.), Academic Press (In Press).

18. Douglass, D. L. and T. W. Barbee: J. Mat. Sci, 4: 121 (1969).

19. Carpenter, R. W.: Acta Met., 15: 1297 (1967).

20. Richman, R. H. and R. G. Davies: Trans. AIME, 236: 1551 (1966).

21. Saito, K, and R. Watanabe: J. Phys. Soc., Japan, 22: 681 (1967).

22. Badia, F. A., G. N. Kirby and J. R. Mihalison: Trans. ASM, 60: 395 (1967).

23. Schwartz, L. H., S. Mahajan and J. T. Plewes : Acta Met., 22: 601 (1974).

24. Dahlgren, S. D.: Ph.D. Thesis, University of California, Berkeley, Lawrence Berkeley Laboratory Report #UCRL 16846 (1966).

25. Bouchard, M., R. J. Livak and G. Thomas: Surface Science, 31: 275 (1972).

26. Brown, L. M. and R. K. Ham: "Strengthening Methods in Crystals", A. Kelly and R. B. Nicholson (eds.) p. 9, Elsevier Publishing Co., 1971.

27. Rao, B. V. N. and G. Thomas; Mat. Sci and Engin., 20: 195 (1975).

28. McMahon, J. M. and G. Thomas: "Microstructure and Design of Alloys", Inst. of Metals, London 1: 180 (1973).

29. G. R. Speich and A. Szirmae:Trans. AIME, 245: 1063 (1969).

30. Brobst, R. P. and G. Krauss: Met. Trans., 5: 457 (1974).

31. Clark , R. A. and G. Thomas: Met. Trans., 6A: 969 (1975).

32. Rao, B.V.N., J.-Y. Koo and G. Thomas: Proc. 33rd EMSA Conference, p. 30, Claitors Publishers, 1975.

33. Lai, G. Y., W. E. Wood, R. A. Clark , V. F. Zackay, and E R. Parker: Met. Trans., 5: 1663 (1974).

34. Cook, J. and J. E. Gordon: Proc. Roy. Soc, A282: 508 (1964).

35. P. R. Manganon and G. Thomas: Met. Trans., 1: 1577,1587 (1970).

36. R. A. Grange, Met. Trans., 2: 65 (1971).

37. Jin, S., J. W. Morris and V. F. Zackay: Met. Trans., 6A: 141 (1975).

38. Snape, E. and N. L. Church: J. Metals, 23:(1972).

39. Koo, J.-Y. and G. Thomas: To be Published, Lawrence Berkeley Laboratory Report #3980 (1975).

40. Johari, O. and G. Thomas: Trans. ASM, 58: 563 (1965).

41. Cheng, I.-L. and G. Thomas: Met. Trans., 3: 503 (1972).

42. Vercaemer, C. and G. Thomas, Ibid, 3: 2501 (1972).

FIGURE CAPTIONS

Fig. 1. Light optical micrograph of coarsened spinodal structure in 70%Cu/19%Ni/11%Fe after aging for 500 hr at 748°C showing the lamellar structure near the grain boundary. Courtesy R. Gronsky

Fig. 2. Photograph of same alloy as Fig. 1 but aged 10 hrs at 655°C showing enhanced coarsening and boundary migration (in direction of $\vec{g} = 002$). The wavelength at the boundary region is almost 3 times that in the matrix. Note that the copper rich phase is in lighter contrast due to preferential electro-polishing. Courtesy R. Gronsky.

Fig. 3. High voltage electron micrograph (650 kV) of overaged and 10% tensile deformed CuNiFe alloy showing interphase dislocations. These have Burger's vectors of a/2<110>. Some slip dislocations are also visible, especially within the lighter contrast, Cu-poor phase.

Fig. 4. Electron micrograph showing (a) part of a packet of dislocated lath martensite (tough) in Fe/5Ni/0.26C, and (b) twinned martensite (brittle) in fe/6.8Mn/0.24C. Courtesy D. Huang.

Fig. 5 (a) Relationship between plane strain fracture toughness and ultimate tensile strength for two experimental ternary alloy steels developed recently. Note that the Fe/Cr/C steel has superior properties to the Fe/Mo/C steel and to other commercially available high strength steels, and 18Ni maraging alloys. Continuous films of stabilized interlath austenite could be identified in Fe/Cr/C steels whereas in Fe/Mo/C steels the amount, if any, was too small to be identified (Data from References 28,31).

(b) Relation between Charpy impact toughness and ultimate tensile strength for Fe/1%Cr/1%Mo/0.3%C alloys and Fe/Mo/C alloys (from

Reference 31). The Fe/Mo/C alloys have low impact toughness at all strength levels while the Fe/1Cr/1Mo/0.3C alloys had good combinations of strength and toughness. Extensive inter-lath retained austenite films (see Fig. 12) were observed by transmission electron microscopy whereas in the Fe/Mo/C alloys none was detected. This diagram also shows the effect of grain refinement for improving the properties. Courtesy Y.-L. Chen.

Fig. 6. Diagram showing schematically the composition-wavelength variation for a spinodal with unequal volume fractions of the two phases. The change in composition Δc is assumed to vary linearly with change in lattice parameters Δa.

Fig. 7. Diagram showing the interfacial dislocations and a slip plane for a semi-coherent spinodal (fcc system). Slip dislocations travel a maximum distance $\sqrt{2}\lambda$ before interacting again at the interface (assuming $z = \lambda$). The values of p and q are determined by the misfit.

Fig. 8. (a) Optical photomicrograph and (b) electron micrograph of Fe/4Cr/0.4C steel quenched from 1200°C showing intergranular cracks (a) and twinned plates (b).

(c) Optical and (d) electron micrographs showing grain refinement after the double treatment shown in Fig. 9D. Two etchants are needed in (c) to distinguish the grain structure. In (d) dislocated, auto-tempered martensite and interlath retained austenites are resolved (Compare to Fig. 8b). This structure is beneficial and gives toughness - See Figs 9,10. Courtesy B. V. N. Rao

Fig. 9. Carbon in solution and martensite packet size are the two most important parameters influencing intergranular quench cracking in

Fe/4Cr/0.4C steel, viz., an increase in either causes an increase in the transformation strains and the resultant impingement stresses of two growing martensitic packets. Conventional high temperature austenitization followed by quenching (Fig. A) invariably leads to intercrystalline cracking due to the large martensite packet size and the carbon being entirely in solution. After this treatment the steel failed prematurely at 200 ksi and at zero elongation. Conventional grain refinement, involving repeated austenitization and quenching (Fig. B) does not result in any significant improvement in mechanical properties since intergranular cracks produced during first quench-do not heal on subsequent heating. Although the transformation strains are reduced in the interrupted-quenched specimen (Fig. C), the intercrystalline cohesion remains poor because of the large martensite packet size. The specimen after this treatment does, however, yield plastically followed by failure at 270 ksi. When this specimen was re-austenitized at 900°C to refine the grain size (Fig. D), a substantial improvement in mechanical properties is achieved. A tensile strength of 335 ksi and a 6% elongation have been obtained. In this case, although the specimen retained most of the carbon in solution, the much reduced martensite packet size resulted in elimination of intergranular cracks. Courtesy of B. V. N. Rao.

Fig. 10. Relationship between yield strength and Charpy-v-notch energy (a) and plane strain fracture toughness (b) for the martensitic double treatments and single conventional lower bainitic treatments of Fe/4Cr/0.4C steel (see Fig. 9). Courtesy B. V. N. Rao.

Fig. 11. Calculated electron diffraction pattern for martensite in [$\bar{1}11$] with retained austenite and Widmanstatten cementite.

Fig. 12. Bright-field image (a) and dark field image (b) of an Fe/1Cr/1Mo/0.3C steel quenched from 870°C into ice water. Note that the interlath retained austenite films do not show good contrast in the bright field image, but are very clear in the (200)γ dark-field image. This is not always the case, but it serves to illustrate the importance of the proper dark field imaging. Courtesy Y.-L. Chen.

Fig. 13. (a,b) SEM fractographs illustrating improvement in Charpy toughness for Fe/1Cr/1Mo/0.3C steel (a) quenched from 1200°C, σy = 194 ksi Cv = 28 ft-lbs and (b) double treated (grain refined) and quenched σy = 196 ksi Cv = 42 ft-lbs. (c) SEM fractograph showing loss of toughness due to tempered martensite embrittlement due to transformation of austenite producing carbide particles at interlath boundaries; σy = 172 ksi Cv = 14 ft-lbs. As for Fig. 13(a), but after 1 hr 350°C tempering (See Fig. 5b). Courtesy Y.-L. Chen.

Fig. 14. Diagram showing principle of heat-treatment to produce martensite dispersions in ferrite. The conventional grain refining cycling is also shown in comparison to that following two phase annealing. Courtesy J.-Y. Koo.

Fig. 15. Electron micrograph showing dislocated martensite and ferrite in doubly treated "INNA" steel. Some heterogeneous precipitation occurs on dislocations in the ferrite especially after tempering. Courtesy J.-Y. Koo.

Fig. 16. Summary of mechanical properties of "INNA" steel showing influence of volume faction of martensite and grain size. Courtesy J.-Y. Koo.

Fig. 17. Diagram suggesting how multiple phase transformations may be useful to provide maximum dispersion strengthening through dislocation generation (martensite) and precipitation:

1 → 2 conventional martensite,

1 → 3 → 5 conventional ausforming,

1 → 2 → 5 first ausage, and then transform to martensite or first spinodally decompose, to disperse particles in austenite, then quench so as to transform one of the phases to dislocated martensite, and produce dislocation multiplication.

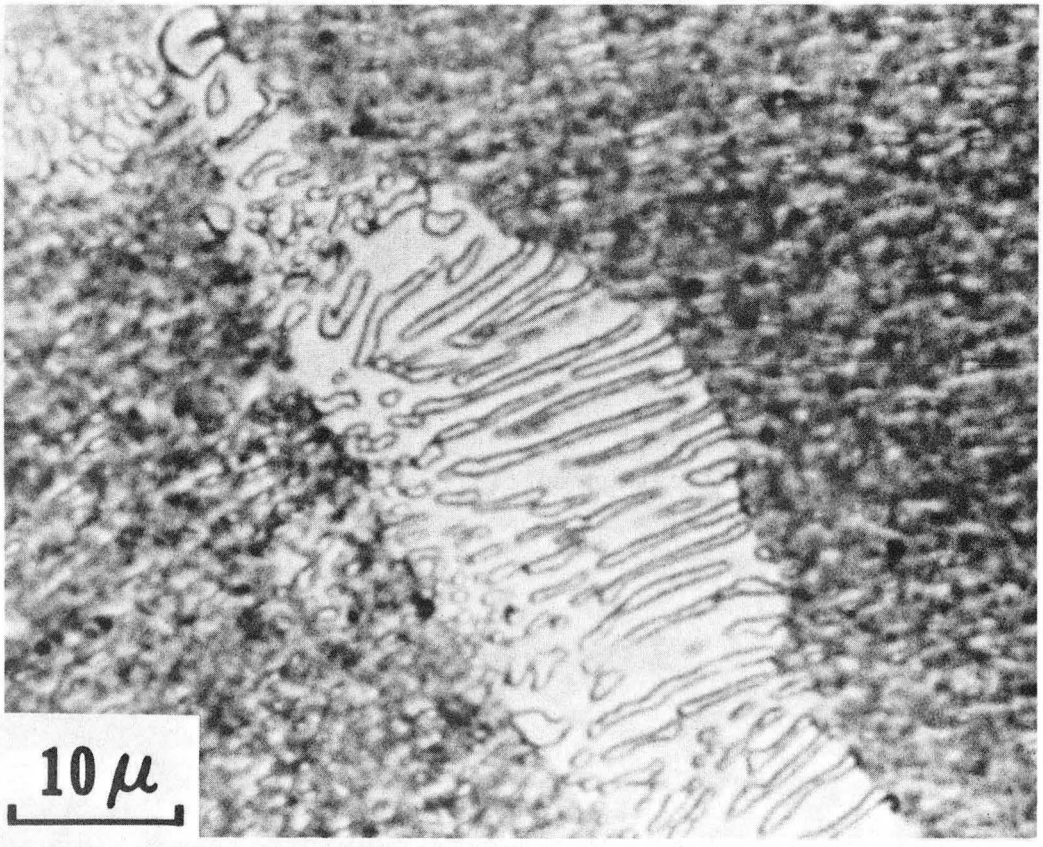

Fig. 1 (XBB 758-6514)

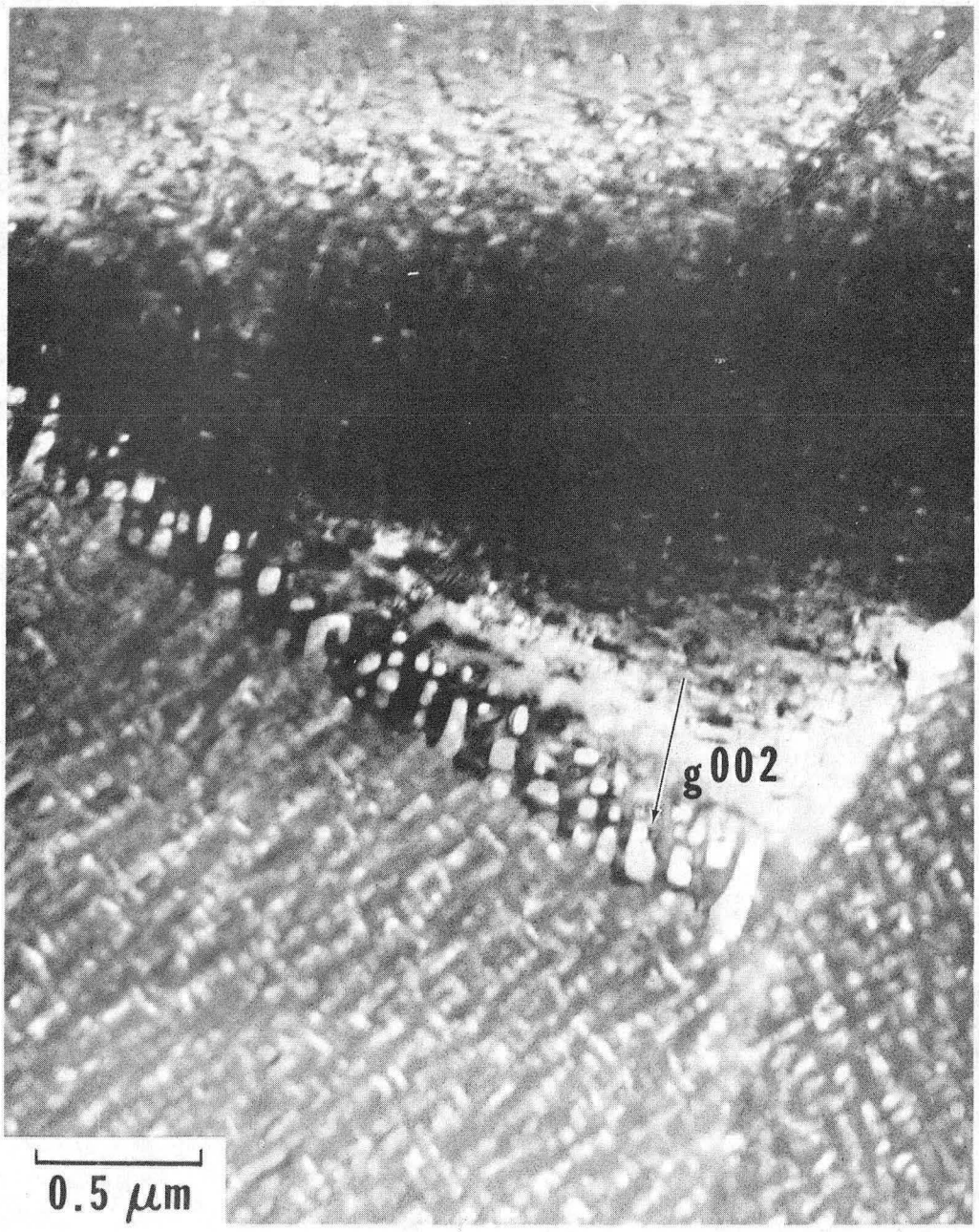

Fig. 2 (XBB 743-1799

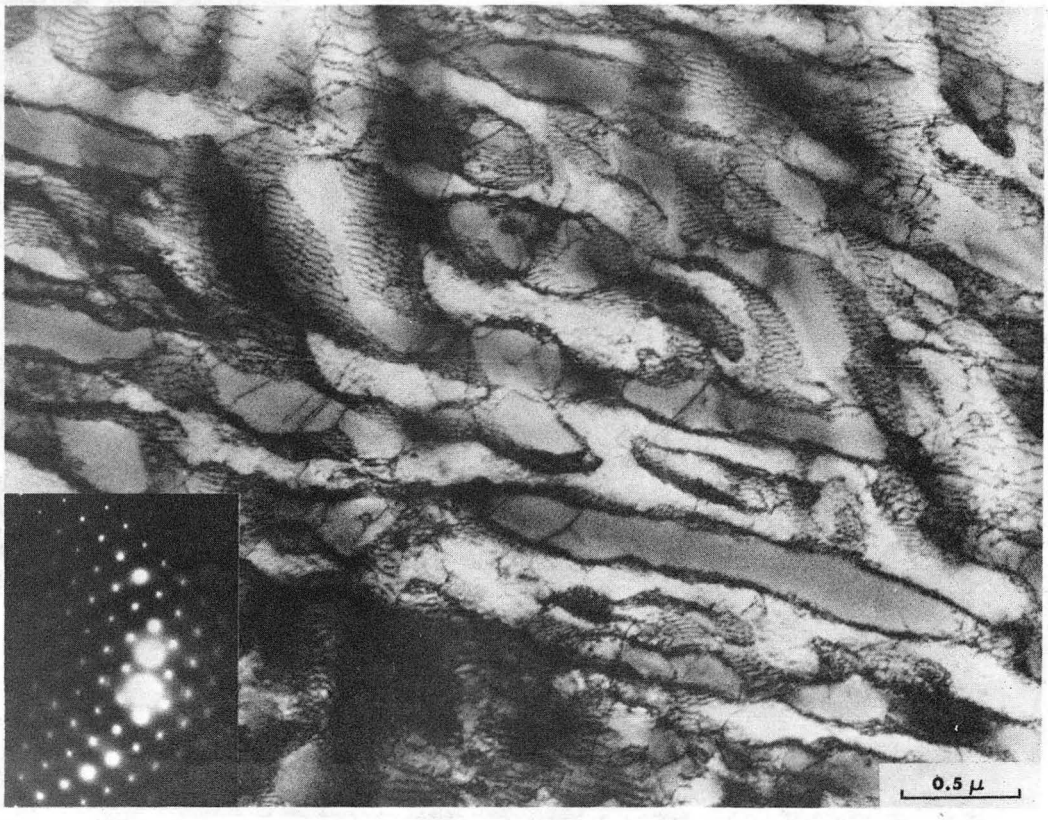

Fig. 3 (XBB 718-3726)

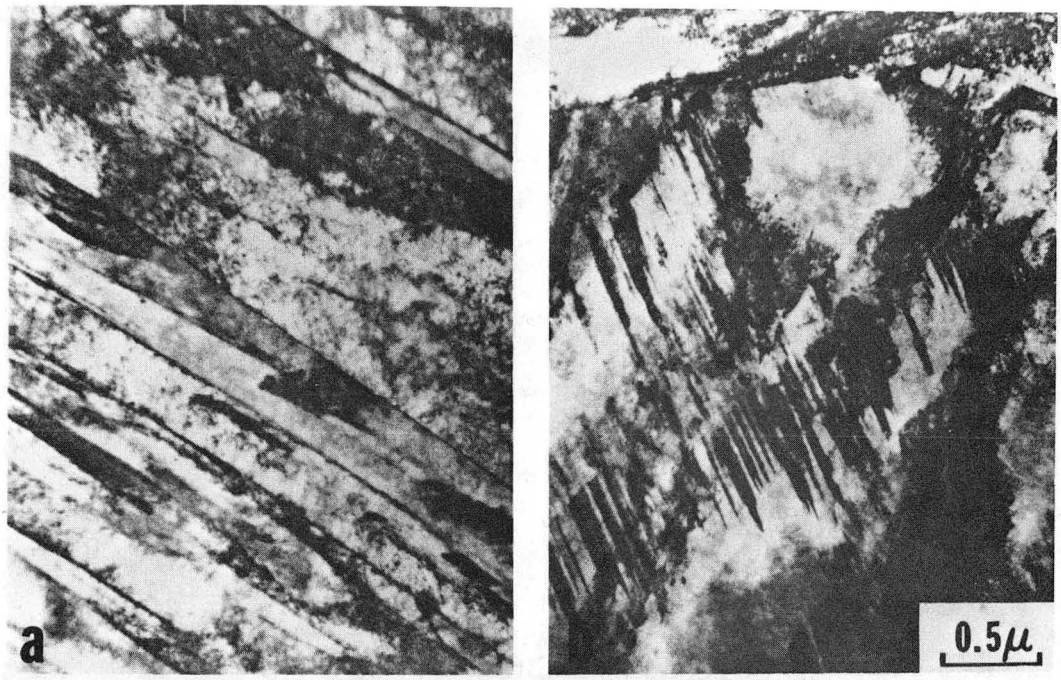

Fig. 4 (XBB 759-6544)

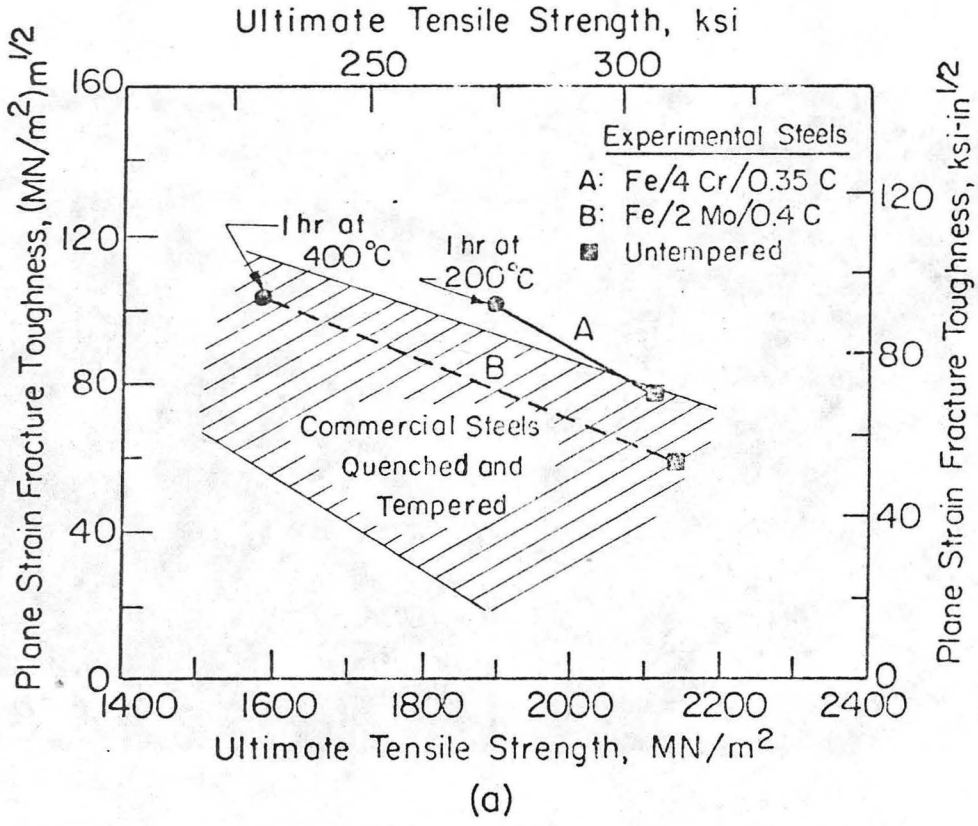

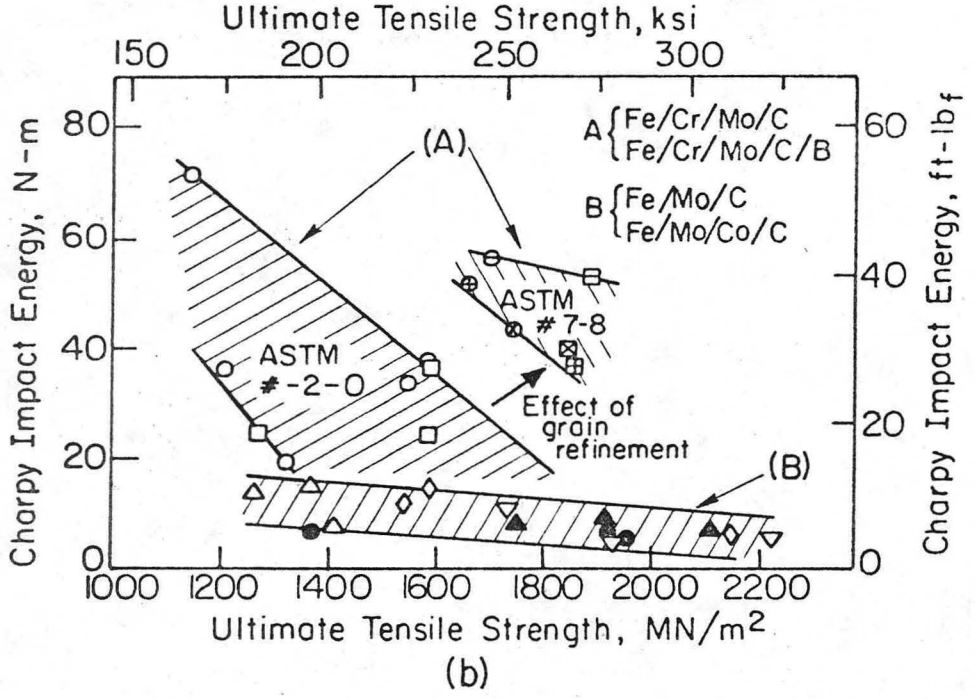

XBL758-6866

Fig. 5

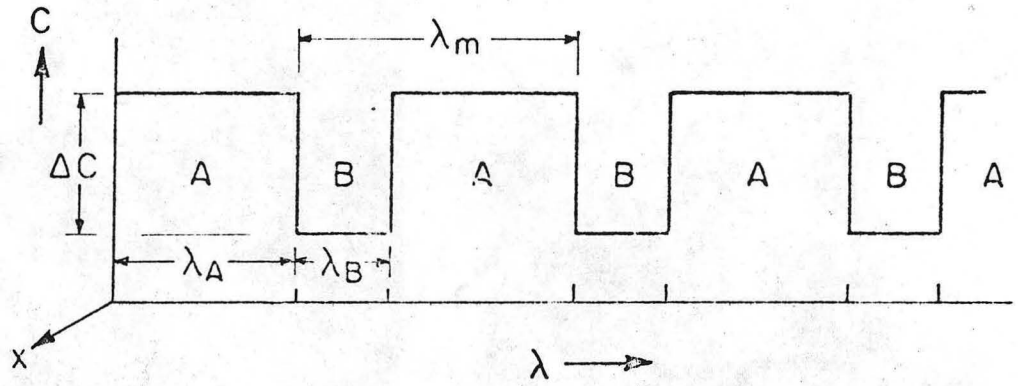
C
λ_m
ΔC
A
B
A
B
A
B
A
λ_A
λ_B
x
λ

Fig. 6

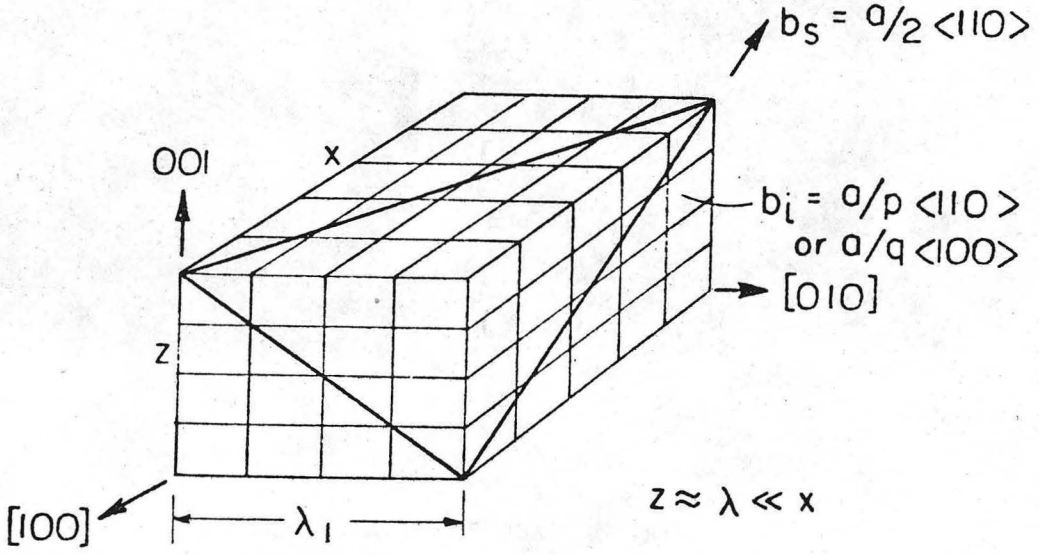
$b_s = a/2 \langle 110 \rangle$
001
x
$b_l = a/p \langle 110 \rangle$
or $a/q \langle 100 \rangle$
[010]
z
[100]
λ_l
$z \approx \lambda \ll x$

Fig. 7

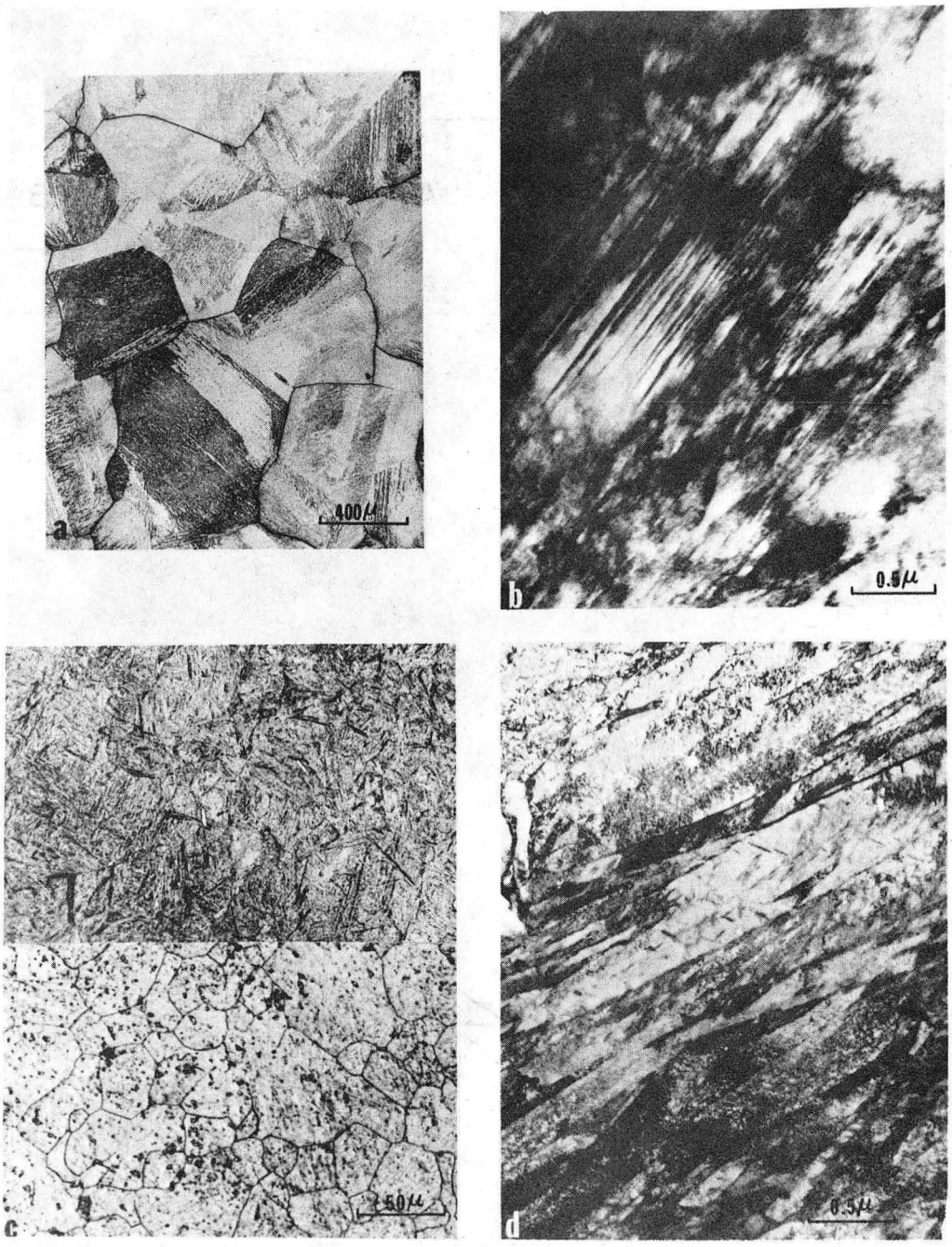

Fig. 8 (XBB 757-5774)

ELIMINATION OF INTERGRANULAR QUENCH CRACKING IN A 0.4% C MARTENSITIC STEEL

SEM FRACTOGRAPH

HEAT-TREATMENT

MECHANICAL PROPERTIES

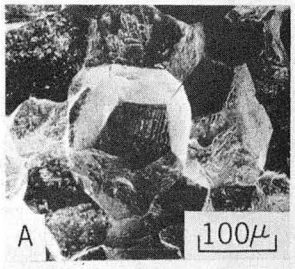

Intergranular fracture in quench-cracked specimens.

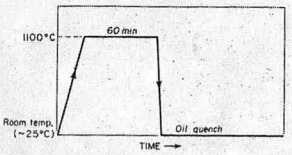

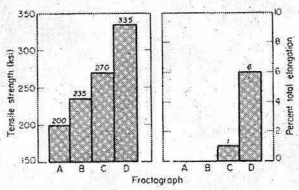

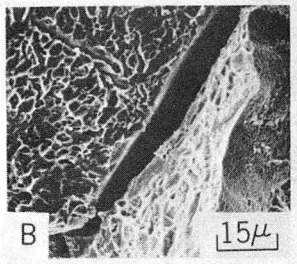

Unhealed intergranular cracks produced after the first quenching. A mixture of intergranular and quasi-cleavage fracture modes are present.

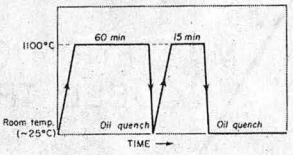

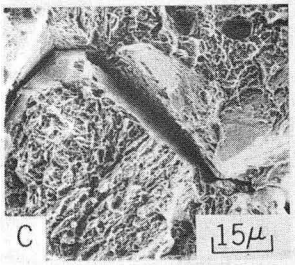

The poor intercrystalline cohesion is evident. A mixed fracture mode consisting of quasicleavage and ductile fracture is obtained in areas where the crack path is transgranular.

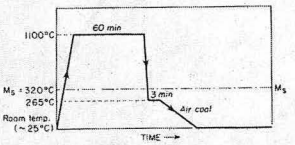

Carbon in solution and martensite packet size are the two most important parameters influencing intergranular quench cracking in Fe/4Cr/0.4C steel, viz., an increase in either of them causes an increase in the transformation strains and the resultant impingement stresses of two growing martensitic packets.

Conventional high temperature austenitization followed by quenching (Fig. A) invariably leads to intercrystalline cracking due to the large martensite packet size and the carbon being entirely in solution. The specimen after this treatment failed prematurely at 200 ksi and at zero elongation.

Conventional grain refinement, involving repeated austenitization and quenching (Fig. B) does not result in any significant improvement in mechanical properties since intergranular cracks produced during first quenching do not heal on subsequent heating.

Although the transformation strains are reduced in the interrupted-quenched specimen (Fig. C), the intercrystalline cohesion remains poor because of the large martensite packet size. The specimen after this treatment does, however, exhibit plastic yielding followed by failure at 270 ksi. When this specimen was re-austenitized at 900°C to refine the grain size (Fig. D), a substantial improvement in mechanical properties is achieved. A tensile strength of 335 ksi and a 6% elongation have been obtained. In this case, although the specimen retained most of the carbon in solution, the much reduced martensite packet size resulted in elimination of intergranular cracks.

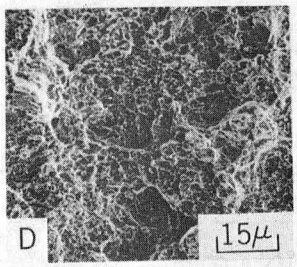

Quench-crack-free specimen showing high energy trans-

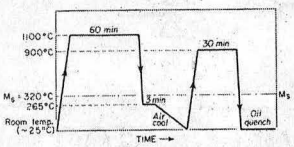

Fig. 9 (XBB 757-5666)

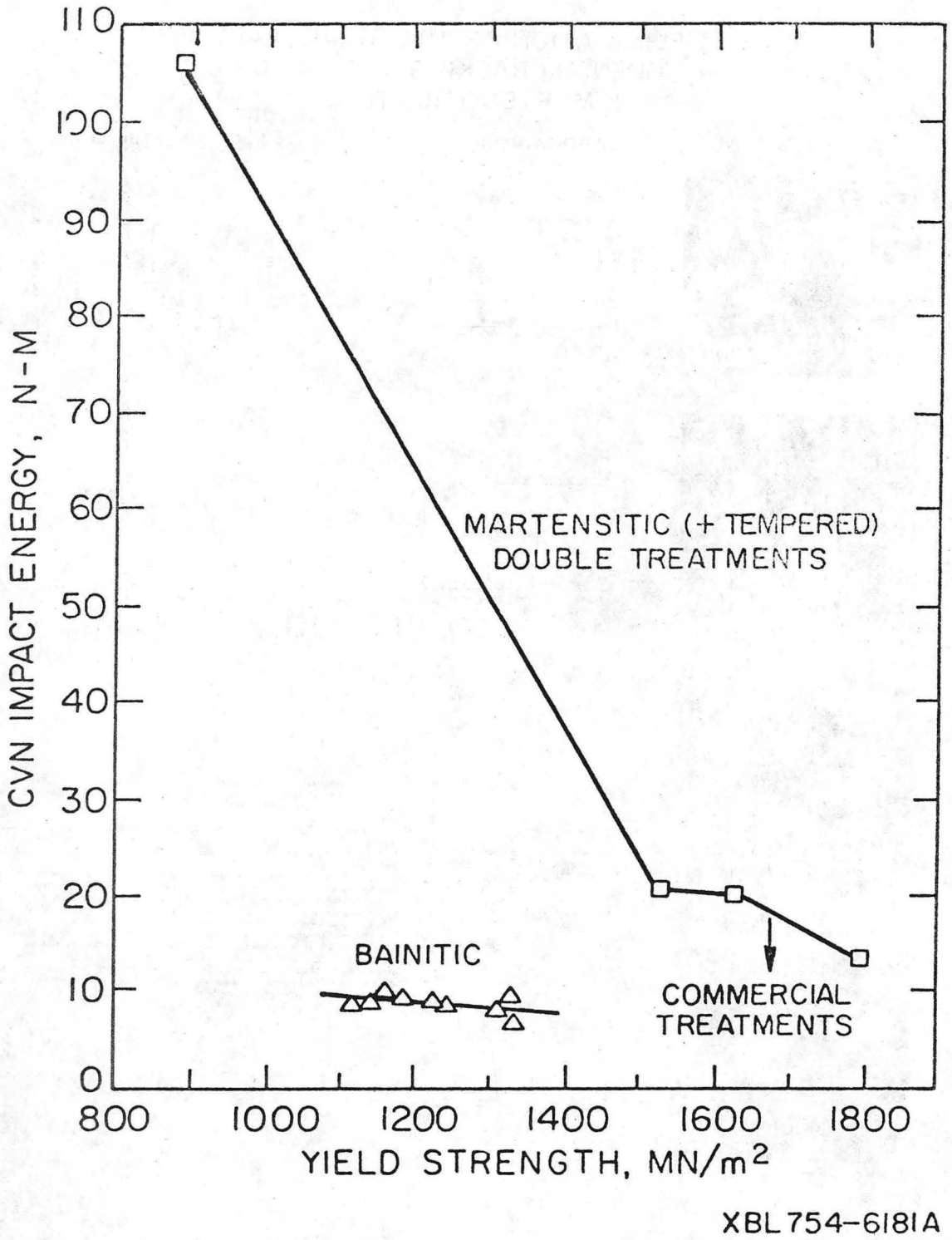
CVN IMPACT ENERGY, N-M
110
100
90
80
70
60
50
40
30
20
10
0
800
1000
1200
1400
1600
1800
YIELD STRENGTH, MN/m2
MARTENSITIC (+ TEMPERED)
DOUBLE TREATMENTS
BAINITIC
COMMERCIAL
TREATMENTS
XBL754-6181A

Fig. 10a

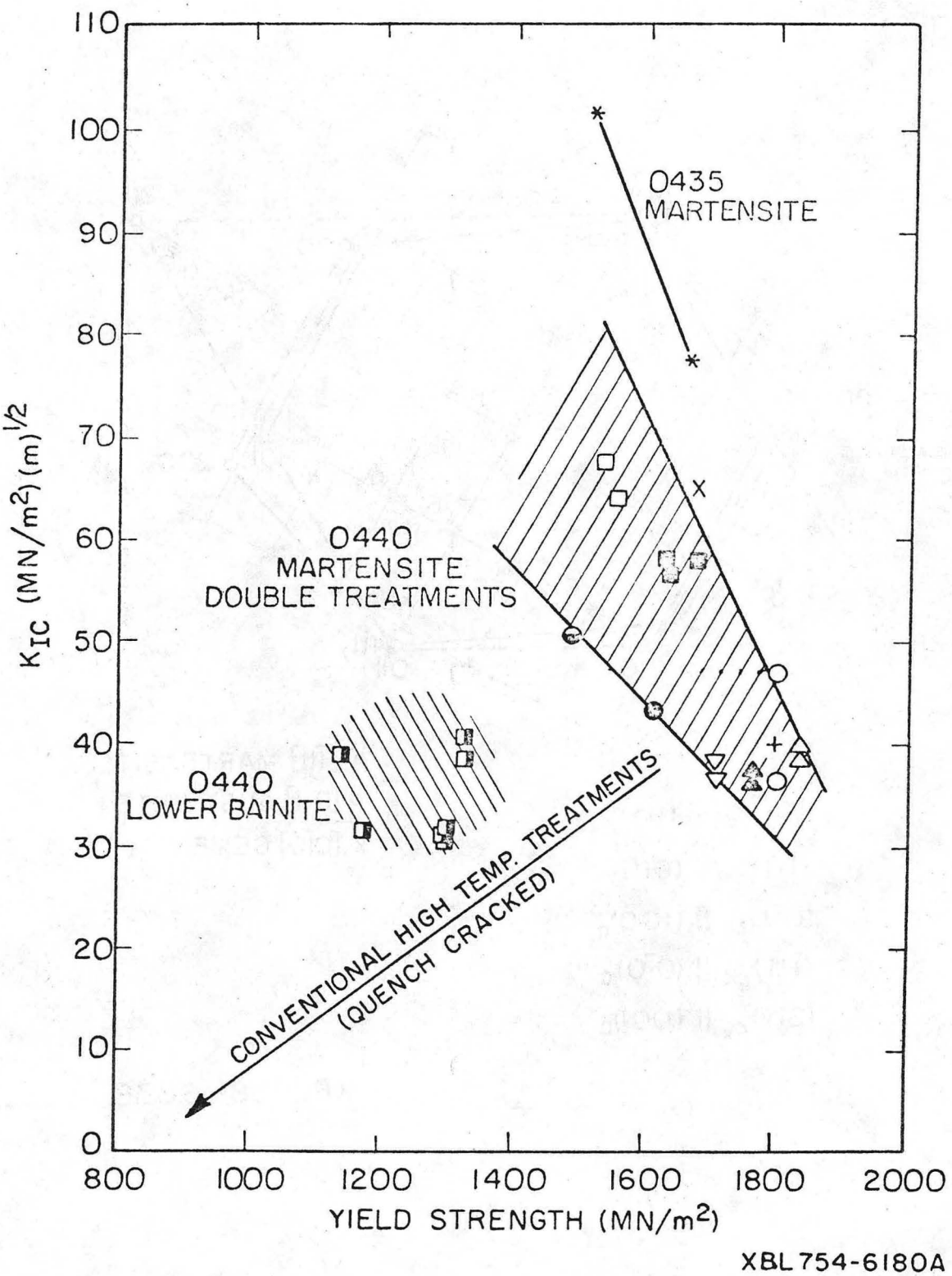

Fig. 10b

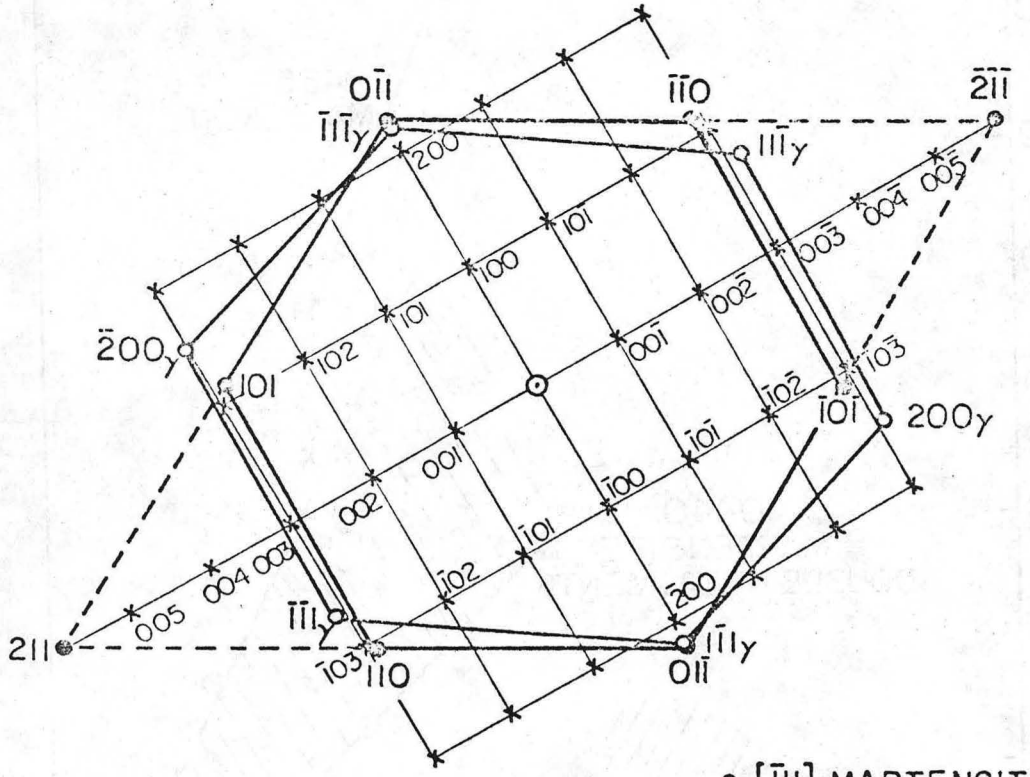

● [$\bar{1}$11] MARTENSITE
o [011] AUSTENITE
x [0$\bar{1}$0] CEMENTITE

$(01\bar{1})_\alpha \parallel (1\bar{1}1)_\gamma$

$(\bar{1}11)_\alpha \parallel (011)_\gamma$

$(0\bar{1}1)_\alpha \parallel (100)_c$

$(\bar{1}11)_\alpha \parallel (0\bar{1}0)_c$

$(211)_\alpha \parallel (001)_c$

XBL758-6830

Fig. 11

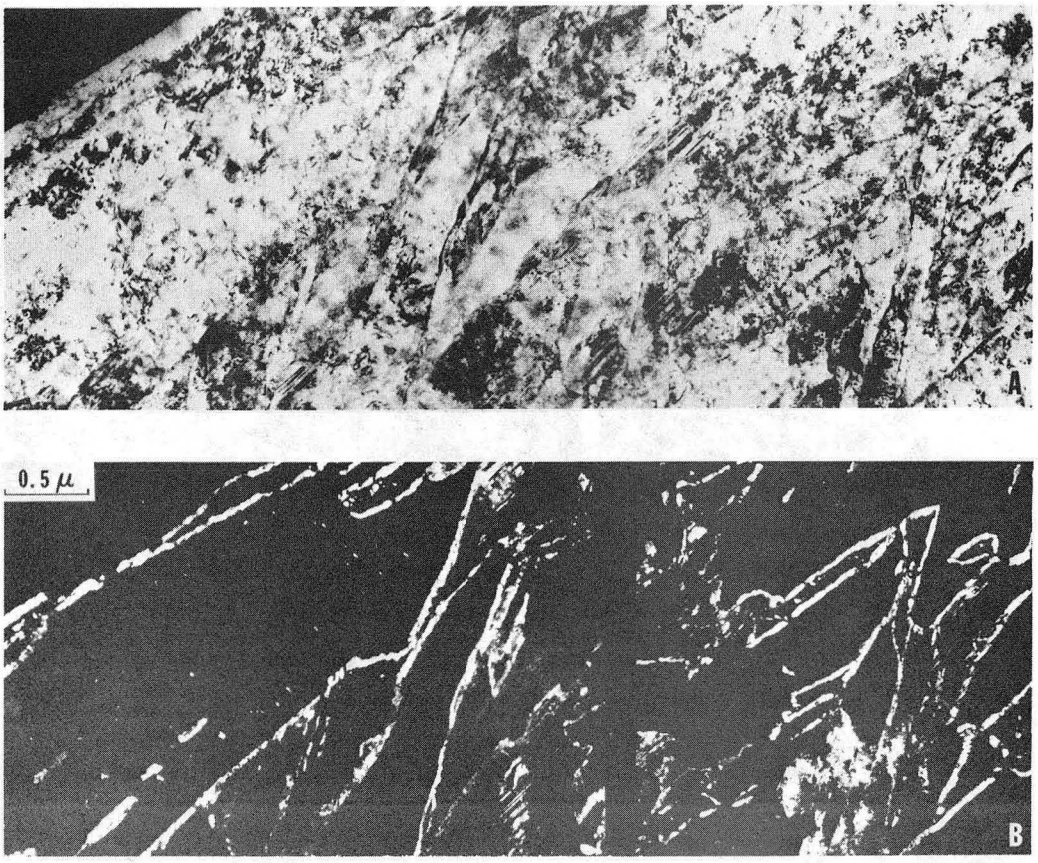

Fig. 12 (XBB 758-5825)

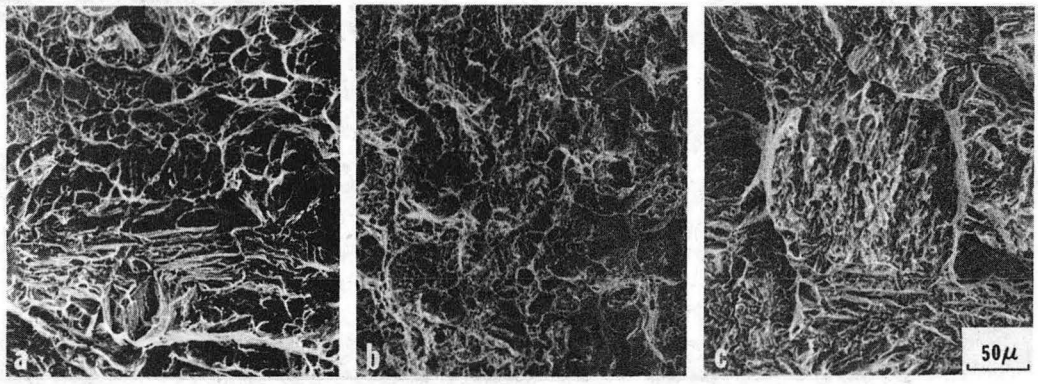

Fig. 13 (XBB 758-6515)

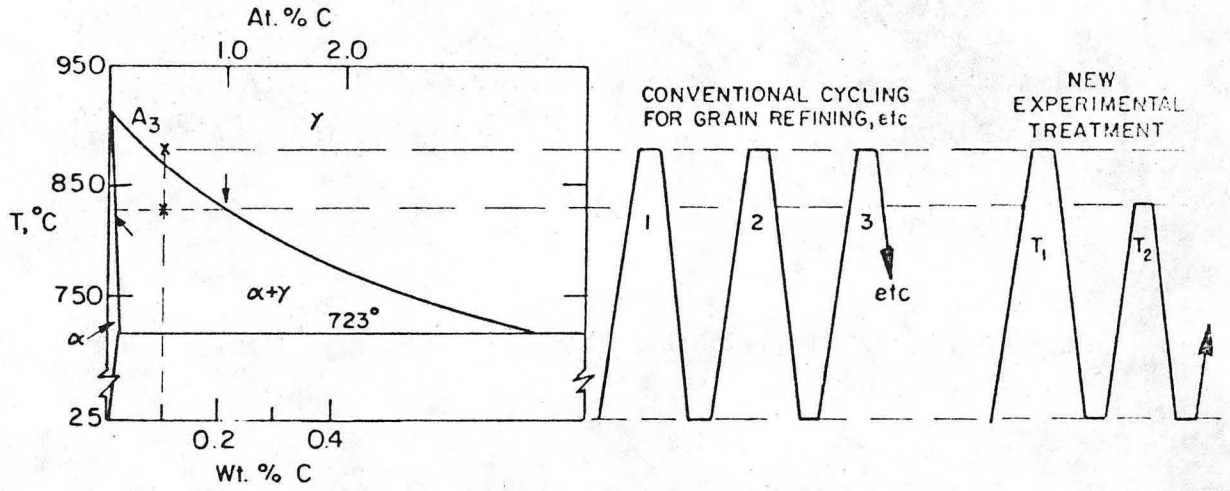

Fig. 14

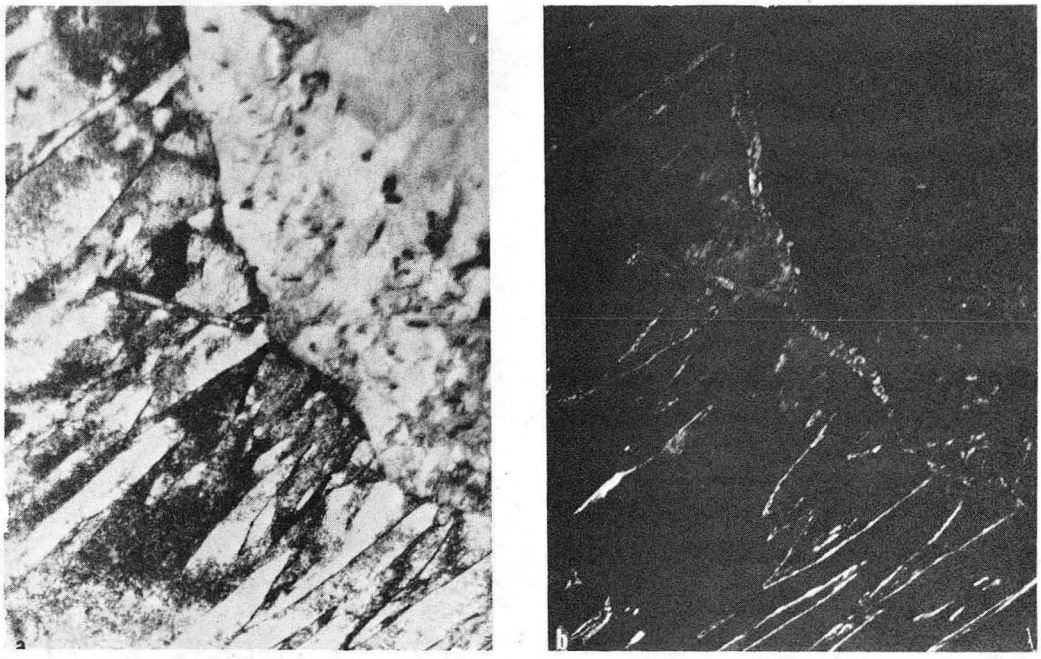

Fig. 15 (XBB 751-755)

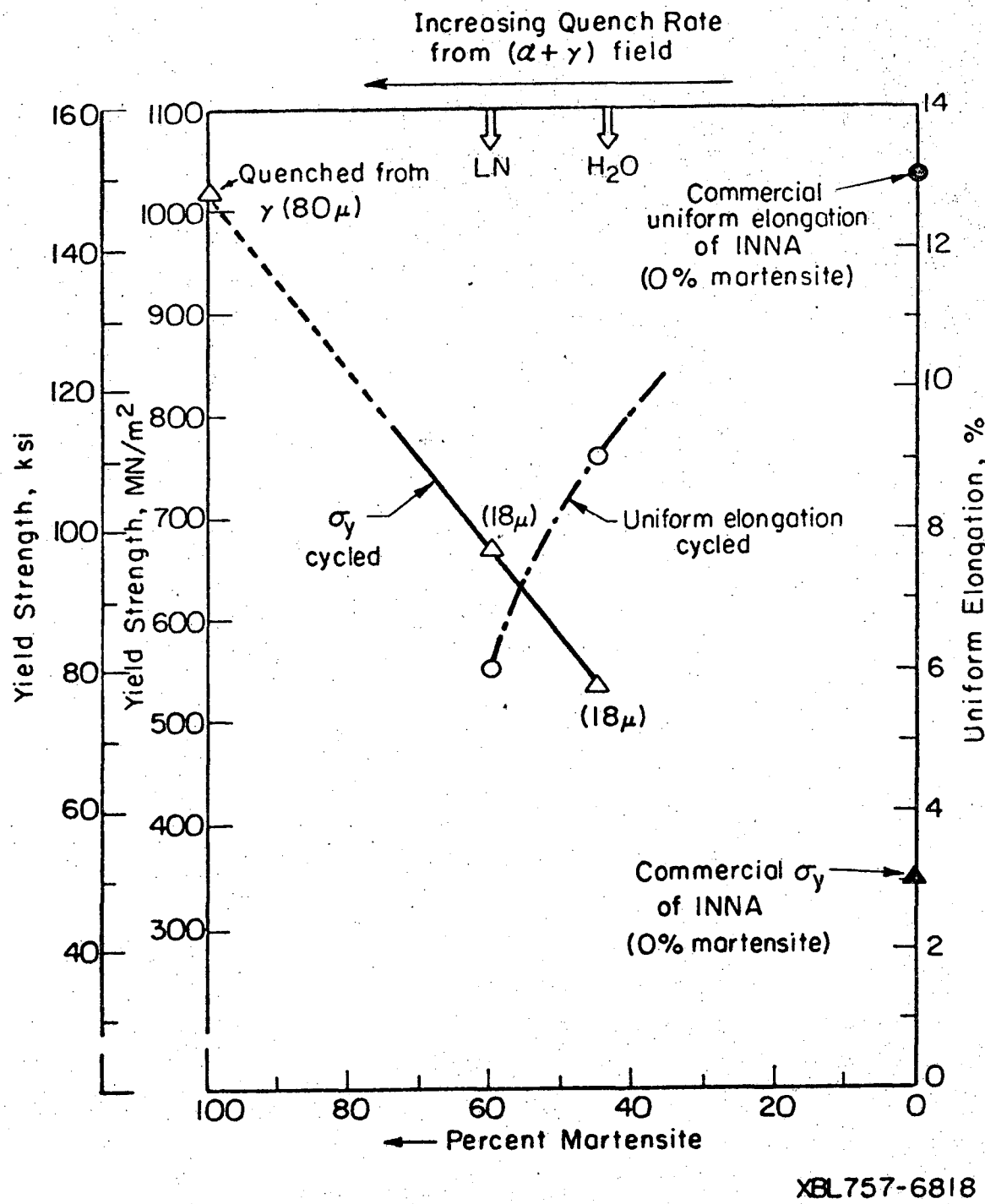

Fig. 16

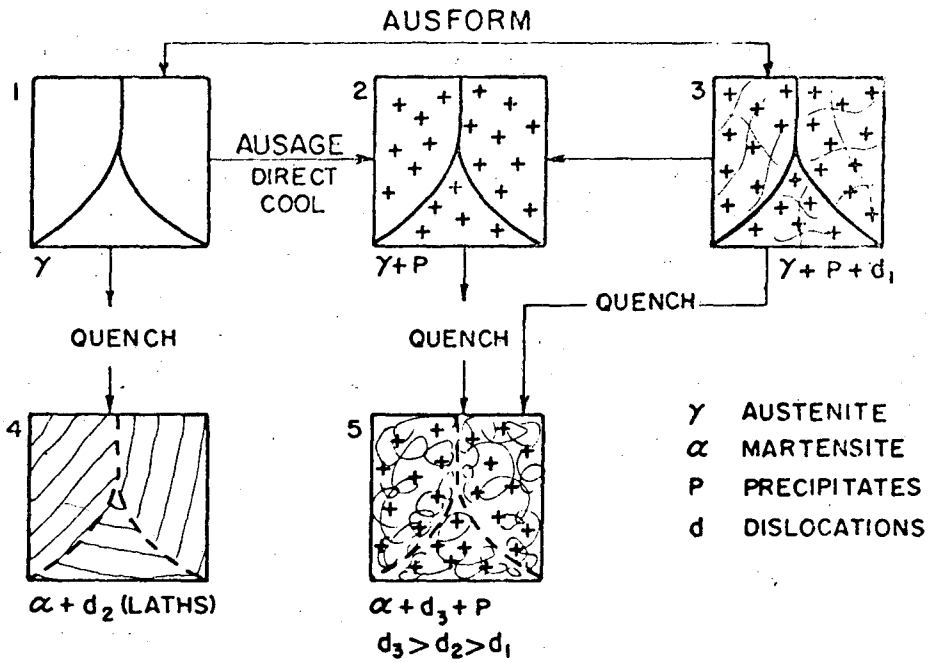

SOME METHODS FOR MAXIMISING SUBSTRUCTURE STRENGTHENING OF MARTENSITE. (G. THOMAS)

XBL 708-1671

Fig. 17

TECHNICAL INFORMATION DIVISION
LAWRENCE BERKELEY LABORATORY
UNIVERSITY OF CALIFORNIA
BERKELEY, CALIFORNIA 94720